



Deposited via The University of Leeds.

White Rose Research Online URL for this paper:

<https://eprints.whiterose.ac.uk/id/eprint/141004/>

Version: Published Version

---

**Article:**

Maters, EC, Delmelle, P, Rossi, MJ et al. (2017) Reactive Uptake of Sulfur Dioxide and Ozone on Volcanic Glass and Ash at Ambient Temperature. *Journal of Geophysical Research: Atmospheres*, 122 (18). 10,077-10,088. ISSN: 2169-897X

<https://doi.org/10.1002/2017JD026993>

---

©2017. American Geophysical Union. All Rights Reserved. Reproduced in accordance with the publisher's self-archiving policy.

**Reuse**

Items deposited in White Rose Research Online are protected by copyright, with all rights reserved unless indicated otherwise. They may be downloaded and/or printed for private study, or other acts as permitted by national copyright laws. The publisher or other rights holders may allow further reproduction and re-use of the full text version. This is indicated by the licence information on the White Rose Research Online record for the item.

**Takedown**

If you consider content in White Rose Research Online to be in breach of UK law, please notify us by emailing [eprints@whiterose.ac.uk](mailto:eprints@whiterose.ac.uk) including the URL of the record and the reason for the withdrawal request.

## RESEARCH ARTICLE

10.1002/2017JD026993

## Key Points:

- Sulfur dioxide and ozone are taken up on volcanic glass/ash at ambient temperature likely at basic and reducing surface sites, respectively
- A typically lower ash reactivity toward these gases may reflect exposure to acidic and oxidizing conditions in the volcanic plume/cloud
- Measured uptake capacity and coefficient values suggest that ash emissions may represent a sink for atmospheric sulfur dioxide and ozone

## Supporting Information:

- Supporting Information S1

## Correspondence to:

E. C. Maters,  
elena.maters@univ-littoral.fr

## Citation:

Maters, E. C., Delmelle, P., Rossi, M. J., & Ayris, P. M. (2017). Reactive uptake of sulfur dioxide and ozone on volcanic glass and ash at ambient temperature. *Journal of Geophysical Research: Atmospheres*, 122, 10,077–10,088, <https://doi.org/10.1002/2017JD026993>

Received 24 APR 2017

Accepted 28 AUG 2017

Accepted article online 31 AUG 2017

Published online 18 SEP 2017

## Reactive Uptake of Sulfur Dioxide and Ozone on Volcanic Glass and Ash at Ambient Temperature

Elena C. Maters<sup>1,2</sup> , Pierre Delmelle<sup>1</sup> , Michel J. Rossi<sup>3</sup> , and Paul M. Ayris<sup>4</sup>

<sup>1</sup>Environmental Sciences, Earth and Life Institute, Université catholique de Louvain, Louvain-la-Neuve, Belgium, <sup>2</sup>Now at Laboratoire de Physico-Chimie de l'Atmosphère, Université du Littoral Côte d'Opale, Dunkirk, France, <sup>3</sup>Laboratory of Atmospheric Chemistry, Paul Scherrer Institute, Villigen, Switzerland, <sup>4</sup>Department of Earth and Environmental Sciences, Ludwig-Maximilian University of Munich, Munich, Germany

**Abstract** The atmospheric impacts of volcanic ash from explosive eruptions are rarely considered alongside those of volcanogenic gases/aerosols. While airborne particles provide solid surfaces for chemical reactions with trace gases in the atmosphere, the reactivity of airborne ash has seldom been investigated. Here we determine the total uptake capacity ( $N_i^M$ ) and initial uptake coefficient ( $\gamma_M$ ) for sulfur dioxide ( $\text{SO}_2$ ) and ozone ( $\text{O}_3$ ) on a compositional array of volcanic ash and glass powders at  $\sim 25^\circ\text{C}$  in a Knudsen flow reactor. The measured ranges of  $N_i^{\text{SO}_2}$  and  $\gamma_{\text{SO}_2}$  ( $10^{11}$ – $10^{13}$  molecules  $\text{cm}^{-2}$  and  $10^{-3}$ – $10^{-2}$ ) and  $N_i^{\text{O}_3}$  and  $\gamma_{\text{O}_3}$  ( $10^{12}$ – $10^{13}$  molecules  $\text{cm}^{-2}$  and  $10^{-3}$ – $10^{-2}$ ) are comparable to values reported for mineral dust. Differences in ash and glass reactivity toward  $\text{SO}_2$  and  $\text{O}_3$  may relate to varying abundances of, respectively, basic and reducing sites on these materials. The typically lower  $\text{SO}_2$  and  $\text{O}_3$  uptake on ash compared to glass likely results from prior exposure of ash surfaces to acidic and oxidizing conditions within the volcanic eruption plume/cloud. While sequential uptake experiments overall suggest that these gases do not compete for reactive surface sites,  $\text{SO}_2$  uptake forming adsorbed S(IV) species may enhance the capacity for subsequent  $\text{O}_3$  uptake via redox reaction forming adsorbed S(VI) species. Our findings imply that ash emissions may represent a hitherto neglected sink for atmospheric  $\text{SO}_2$  and  $\text{O}_3$ .

## 1. Introduction

The average annual load of volcanic ash to the atmosphere ( $176$ – $256 \text{ Tg a}^{-1}$ ) (Durant et al., 2010) provides a total solid surface area on the order of  $1.8$  to  $2.6 \times 10^8 \text{ km}^2$  (assuming an ash specific surface area of  $1 \text{ m}^2 \text{ g}^{-1}$ ) (Delmelle et al., 2005), equivalent to one third to one half of the Earth's geometric surface area. A single Plinian eruption such as the 1991 Pinatubo eruption generates an ash mass (e.g.,  $\sim 3000 \text{ Tg}$ ) (Koyaguchi, 1996) with a solid surface area reaching over ten times this amount. Maters et al. (2016) have recently confirmed the presence of reactive surface sites on volcanic ash and glass, and similar to wind blown mineral dust from arid and semiarid regions ( $1000$ – $3000 \text{ Tg a}^{-1}$  emitted) (Matsuki et al., 2005; Penner et al., 2001; Usher et al., 2003), airborne ash surfaces may take part in heterogeneous reactions with trace atmospheric gases such as  $\text{SO}_2$ ,  $\text{O}_3$ ,  $\text{NO}_x$ , and organic compounds.

While the impact of volcanic activity on atmospheric chemistry is traditionally studied in relation to sulfur and halogen emissions (e.g., Brasseur et al., 1990; Robock, 2000; von Glasow et al., 2009), the potential of aluminosilicate ash from explosive eruptions to influence atmospheric chemistry remains unknown. Amid growing recognition of  $\text{O}_3$  depletion in the vertical volcanic plume and/or the laterally dispersed volcanic cloud (e.g., Roberts et al., 2009; Surl et al., 2015; von Glasow, 2010), the role of ash particles has been dismissed (Vance et al., 2010). However, this conclusion was based on an assumed low reactivity of ash toward  $\text{O}_3$  and prompts reconsideration as ash- $\text{O}_3$  interaction has not been investigated before now. Moreover, although it has been suggested that a short residence time of airborne ash limits its atmospheric/climatic impact relative to volcanic gases and aerosols (e.g., Niemeier et al., 2009; Robock, 2000), recent evidence of ash suspended aloft for several months (Vernier et al., 2016) calls for a more careful assessment of its potential effects.

Therefore, in light of the intermittent yet non-negligible presence of ash surfaces in the atmosphere, quantitative constraints on ash-gas reactivity are essential to improve understanding of the capacity of ash to act as a source of/sink for trace atmospheric species. In addition to affecting atmospheric chemistry, heterogeneous reactions can modify the physicochemical characteristics (e.g., hygroscopicity) of particle

**Table 1**  
 Details of the Volcanic Glass and Ash Samples Used in This Study

Sample code	Material							
	Glass				Ash			
	TRB	AND	DCT	RHY	EYJA	TUNG	PIN	CHAI
Source volcano	Etna	Tungurahua	Unzen	Lipari	Eyjafjallajökull	Tungurahua	Pinatubo	Chaitén
Eruption date <sup>a</sup>	-	-	-	-	17 April 2010	23 August 2012	15 June 1991	2 May 2008
Classification <sup>b</sup>	Trachybasalt	Andesite	Dacite	Rhyolite	Trachyandesite	Andesite	Andesite	Rhyolite
SSA <sub>BET</sub> (m <sup>2</sup> g <sup>-1</sup> ) <sup>c</sup>	0.3	0.2	0.3	0.5	7.5	1.8	1.5	0.5
Bulk glass content (wt %) <sup>d</sup>	100	100	100	100	56	45	60	76

<sup>a</sup>The glass samples were generated in the laboratory from volcanic rock (melted, homogenized, quenched, and crushed) and therefore are no longer associated with an individual eruption. <sup>b</sup>According to the Total Alkali Silica diagram (Le Maitre et al., 2002) based on bulk composition (Table S1). <sup>c</sup>Uncertainty in duplicate measurements is  $\pm 5\%$ . <sup>d</sup>Accuracy is estimated to be in the range of 5–10% based on analysis of artificial mixtures comprised of volcanic glass and two crystalline phases.

surfaces, in turn, influencing their impact on radiation, cloud properties, and thereby ultimately climate (e.g., Wurzler et al., 2000). The present study quantifies for the first time the reactivity of volcanic ash toward gaseous SO<sub>2</sub> and O<sub>3</sub> at ambient temperature. Using a low-pressure flow reactor, we determine the total uptake capacity and initial uptake coefficient of SO<sub>2</sub> and O<sub>3</sub> on a compositional array of natural ash and synthetic aluminosilicate glass powders, the glass serving as a proxy for the dominant constituent of ash.

## 2. Materials and Methods

### 2.1. Volcanic Glass and Ash Samples

Eight powdered glass and ash samples from trachybasaltic to rhyolitic in composition, broadly spanning a range of compositions produced during volcanic activity, were used in this study (Table 1). Details on the origin of these materials and on their physicochemical characterization are given in Maters et al. (2016). The surface elemental composition of the samples is provided in the supporting information (SI; Table S1).

### 2.2. Knudsen Flow Reactor Experiments

Ash is exposed to magmatic SO<sub>2</sub> within the volcanic eruption plume/cloud as well as atmospheric SO<sub>2</sub> upon mixing with ambient air. The latter process also brings ash into contact with atmospheric oxidizing agents such as O<sub>3</sub>. Thus, measurements of SO<sub>2</sub> and O<sub>3</sub> uptake in isolation and in sequence (SO<sub>2</sub> followed by O<sub>3</sub>) on the glass and ash material were carried out.

All experiments were conducted at ambient temperature ( $\sim 25^\circ\text{C}$ ) in a Knudsen flow reactor operating under high vacuum ( $< 0.1$  Pa) in the molecular flow regime (Caloz et al., 1997; Golden et al., 1973). The key principles of the Knudsen apparatus as applied to study heterogeneous reactions on volcanic glass and ash are described in Maters et al. (2016). Details on the reactor parameters and the experimental protocol used for uptake measurements appear in the SI (Table S2 and Text S2). Briefly, the technique relies on measuring the rate of gas disappearance when exposed to a substrate (here a powdered solid) within the reactor relative to the rate of gas effusion from the reactor through an escape aperture. An experiment involves recording the mass spectrometer signal intensity of a parent or fragment ion before, during, and after gas exposure to the substrate.

The total number of gas molecules  $M$  taken up on the sample  $N_i^M$  is calculated according to

$$N_i^M = \int (F_i^M - F^M(t)) dt \quad (\text{integration limits between } t_0 \text{ and } t_s) \quad (1)$$

where  $F_i^M$  and  $F^M(t)$  correspond to the measured molecular flow rates of the gas entering and exiting the reactor, respectively, and the integration period from  $t_0$  to  $t_s$  represents the time interval taken for the gas to saturate the sample surface, i.e., when the experimentally measured uptake becomes negligible and  $F_i^M = F^M(t)$ . The calculated  $N_i^M$  value is normalized by the Brunauer-Emmett-Teller (BET) surface area (calculated from the BET specific surface area; Table 1) of the sample in order to give number of gas molecules taken up per square centimeter of its surface (i.e., to account for differences in the total available area presented by the sample surfaces).

The reaction kinetics can be represented in two ways assuming a first-order rate law for adsorption. The first is a heterogeneous rate constant  $k_{het}$ , which depends on the effusion rate constant  $k_{esc}$  and is unique to the specific measurement system, whereas the second is a dimensionless uptake probability or coefficient  $\gamma_M$ , which has been normalized by the surface-to-volume ratio  $A_s/V$  of the system and is therefore a transferable parameter. The uptake coefficient is defined as the fractional collision probability of gas molecule M loss to the sample surface per unit time. These kinetic parameters are calculated as follows:

$$k_{het} = (I_o/I-1)/k_{esc} \tag{2}$$

$$\gamma_M = k_{het}/\omega = (I_o/I-1)(A_h/A_s) = k_{het}4V/(cA_s) \tag{3}$$

where  $I_o$  and  $I$  are the measured amplitudes of the mass spectrometer signal when the sample is isolated and exposed, respectively,  $A_h$  is the surface area of the escape aperture,  $A_s$  is the geometric surface area of the sample plate,  $V$  is the volume of the flow reactor, and  $\omega$  is the collision frequency of the average gas molecule moving at a mean molecular speed  $c$  with the sample surface.

### 3. Results

The mass spectrometer signal intensity for  $SO_2$  or  $O_3$  immediately decreased upon gas exposure to the glass or ash material and then recovered over tens of seconds to several minutes toward a steady state level equivalent to the initial signal intensity (e.g., Figures 1a and 1b).

#### 3.1. Sulfur Dioxide Uptake

The total number of  $SO_2$  molecules taken up per unit surface area ( $N_i^{SO_2}$ ) and the initial  $SO_2$  uptake coefficient ( $\gamma_{SO_2}$ ) of the glass and ash samples in each experiment are listed in Table S3.

##### 3.1.1. Total $SO_2$ Uptake Capacity

Values of  $N_i^{SO_2}$  for each sample are displayed as a function of surface Si content in Figure 2a. The glass samples exhibited  $N_i^{SO_2}$  values on the order of  $10^{13}$  molecules  $cm^{-2}$ , with the lowest and highest corresponding to the compositional end-members rhyolite and trachybasalt glass ( $0.8$ – $1.6$  and  $5.7$ – $6.3 \times 10^{13}$  molecules  $cm^{-2}$ , respectively). The ash samples exhibited  $N_i^{SO_2}$  values ranging from middle  $10^{11}$  to low  $10^{13}$  molecules  $cm^{-2}$ , with the lowest corresponding to Chaitén and Tungurahua ash ( $5.8$ – $6.2$  and  $5.9$ – $12 \times 10^{11}$  molecules  $cm^{-2}$ , respectively) and highest corresponding to Pinatubo and Eyjafjallajökull ash ( $3.9$ – $6.7 \times 10^{12}$  and  $1.2$ – $1.8 \times 10^{13}$  molecules  $cm^{-2}$ , respectively).

##### 3.1.2. Initial $SO_2$ Uptake Coefficient

Values of  $\gamma_{SO_2}$  for each sample are shown as a function of surface Si content in Figure 2b. Within the glass data set, the rhyolite and trachybasalt glass compositional end-members displayed the lowest and highest  $\gamma_{SO_2}$  values ( $1.0$ – $1.7$  and  $3.6$ – $4.5 \times 10^{-2}$ , respectively), although the former range is nearly indistinguishable from

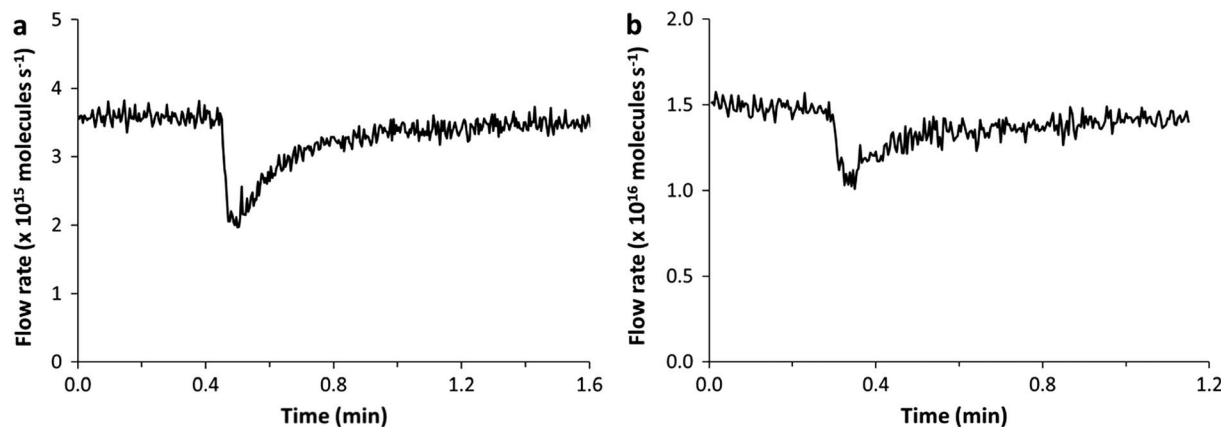


**Figure 1.** Mass spectrometer signal intensity (a) at  $m/e$  64 as a function of time during exposure of 248 mg of andesite glass to  $SO_2$  gas at a concentration of  $1.6 \times 10^{12}$  molecules  $cm^{-3}$  and (b) at  $m/e$  48 as a function of time during exposure of 130 mg of Eyjafjallajökull ash to  $O_3$  gas at a concentration of  $6.0 \times 10^{12}$  molecules  $cm^{-3}$ .

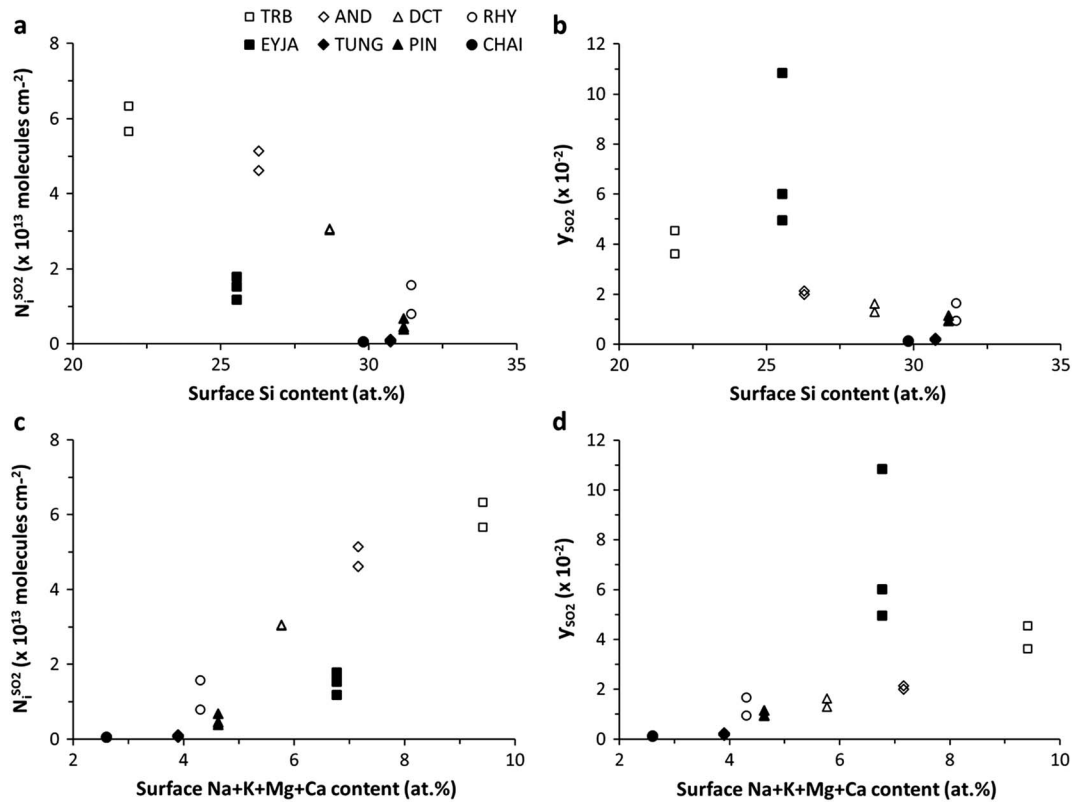


**Figure 2.** (a) Total SO<sub>2</sub> uptake capacity ( $N_i^{SO_2}$ ) and (b) initial SO<sub>2</sub> uptake coefficient ( $\gamma_{SO_2}$ ) versus surface Si content of the glass and ash samples. (c) Total SO<sub>2</sub> uptake capacity ( $N_i^{SO_2}$ ) and (d) initial SO<sub>2</sub> uptake coefficient ( $\gamma_{SO_2}$ ) versus surface Na + K + Mg + Ca content of the glass and ash samples. TRB: trachybasalt glass, AND: andesite glass, DCT: dacite glass, RHY: rhyolite glass. EYJA: Eyjafjallajökull ash, TUNG: Tungurahua ash, PIN: Pinatubo ash, CHAI: Chaitén ash.

that of the dacite glass. Within the ash data set, the Pinatubo and Eyjafjallajökull ash displayed the highest  $\gamma_{SO_2}$  values (0.9–1.1 and  $5.0$ – $10.8 \times 10^{-2}$ , respectively); comparable to the range exhibited by the glass material. In contrast, the Chaitén and Tungurahua ash  $\gamma_{SO_2}$  values ( $1.3$ – $1.5$  and  $1.6$ – $2.4 \times 10^{-3}$ , respectively) were up to an order of magnitude lower.

### 3.2. Ozone Uptake

The total number of O<sub>3</sub> molecules taken up per unit surface area ( $N_i^{O_3}$ ) and the initial O<sub>3</sub> uptake coefficient ( $\gamma_{O_3}$ ) of the glass and ash material in each experiment are given in Table S4.

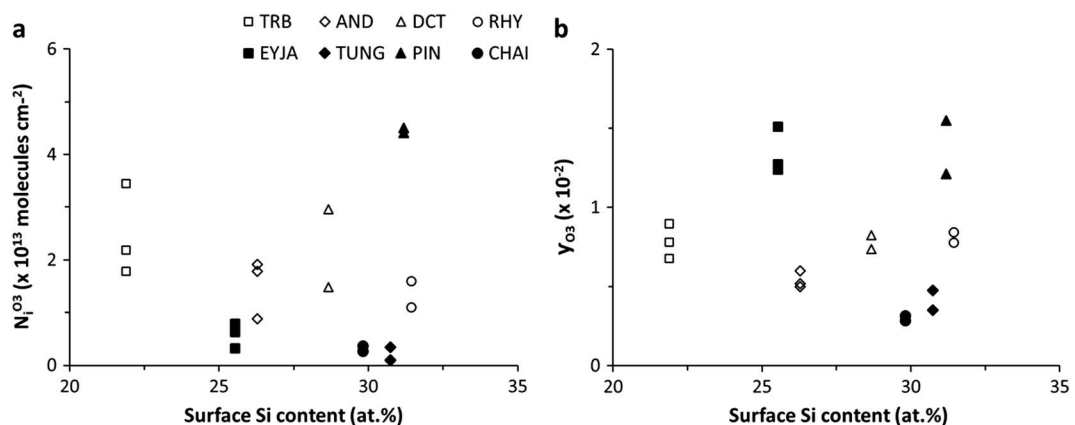


**Figure 3.** (a) Total O<sub>3</sub> uptake capacity ( $N_i^{O_3}$ ) and (b) initial O<sub>3</sub> uptake coefficient ( $\gamma_{O_3}$ ) versus surface Si content of the glass and ash samples. Sample codes as in Figure 2.

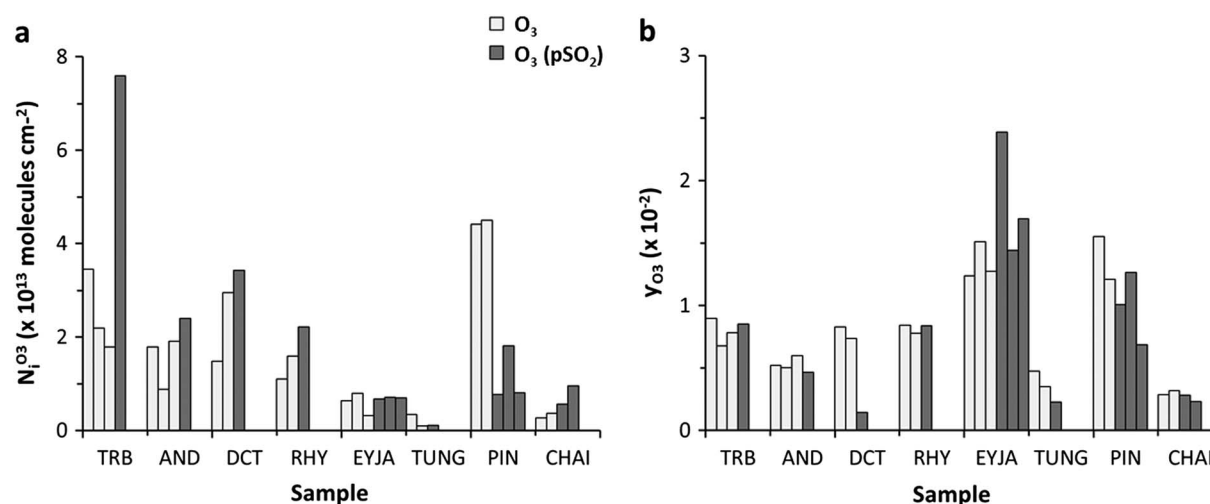


**Figure 4.** (a) Total  $\text{O}_3$  uptake capacity ( $N_i^{\text{O}_3}$ ) and (b) initial  $\text{O}_3$  uptake coefficient ( $\gamma_{\text{O}_3}$ ) for the original and  $\text{SO}_2$  pre-exposed ( $\text{pSO}_2$ ) glass and ash samples. Sample codes as in Figure 2.

### 3.2.1. Total $\text{O}_3$ Uptake Capacity

Values of  $N_i^{\text{O}_3}$  for each sample are presented as a function of surface Si content in Figure 3a. The  $N_i^{\text{O}_3}$  values range from  $0.9$  to  $3.4 \times 10^{13}$  molecules  $\text{cm}^{-2}$  for the glass and  $0.9$  to  $7.9 \times 10^{12}$  molecules  $\text{cm}^{-2}$  for the ash, except Pinatubo ash which displayed the highest  $N_i^{\text{O}_3}$  values of  $4.4$  to  $4.5 \times 10^{13}$  molecules  $\text{cm}^{-2}$  across all samples.

### 3.2.2. Initial $\text{O}_3$ Uptake Coefficient

Values of  $\gamma_{\text{O}_3}$  for each sample are plotted as a function of surface Si content in Figure 3b. All samples exhibited  $\gamma_{\text{O}_3}$  values in the range of low  $10^{-3}$  to low  $10^{-2}$ , with the glass and ash broadly comparable, although Pinatubo and Eyjafjallajökull ash showed notable  $\gamma_{\text{O}_3}$  values up to 6 times greater than those of the other samples.

### 3.3. Ozone Uptake on Sulfur Dioxide-Exposed Samples

The  $N_i^{\text{O}_3}$  and  $\gamma_{\text{O}_3}$  values of the  $\text{SO}_2$ -exposed glass and ash in each experiment are provided in Table S5.

Figure 4a shows the  $N_i^{\text{O}_3}$  values for samples exposed only to  $\text{O}_3$  and those exposed to  $\text{SO}_2$  and subsequently to  $\text{O}_3$ . For the glass samples, previous  $\text{SO}_2$  exposure slightly increased  $N_i^{\text{O}_3}$ , by a factor of 1.5 to 3 on average, but a robust statistical analysis is not possible due to the small sample size. In contrast, previous exposure of the ash samples to  $\text{SO}_2$  did not exert a consistent influence on  $N_i^{\text{O}_3}$ , although Pinatubo ash exhibited a notable decrease by a factor of 4 on average in  $N_i^{\text{O}_3}$  after  $\text{SO}_2$  exposure.

Figure 4b shows the  $\gamma_{\text{O}_3}$  values for samples exposed only to  $\text{O}_3$  and those exposed to  $\text{SO}_2$  and then to  $\text{O}_3$ . Overall, no significant effect of prior  $\text{SO}_2$  exposure on  $\gamma_{\text{O}_3}$  for the glass or ash samples is apparent. However, the dacite glass displayed a decrease by a factor of almost 6 in  $\gamma_{\text{O}_3}$  when previously exposed to  $\text{SO}_2$ .

## 4. Discussion

### 4.1. Sulfur Dioxide Uptake

All volcanic glass and ash samples were reactive toward  $\text{SO}_2$  gas (Table S3).

The  $N_i^{\text{SO}_2}$  of the glass samples decreases with their surface Si content (Figure 2a). The  $\gamma_{\text{SO}_2}$  roughly follows the same tendency (Figure 2b). This conforms with previous findings that gaseous  $\text{SO}_2$  is relatively unreactive toward silica ( $\text{SiO}_2$ ). For example, Usher et al. (2002) measured a lower  $\text{SO}_2$  uptake on  $\text{SiO}_2$  than on  $\text{MgO}$ ,  $\text{Al}_2\text{O}_3$ ,  $\text{Fe}_2\text{O}_3$ , and  $\text{TiO}_2$  mineral powders, whereas Farges et al. (2009) observed no to little  $\text{SO}_2$  adsorption on quartz and pure  $\text{SiO}_2$  glass, in contrast to multicomponent glasses. On the other hand, the  $N_i^{\text{SO}_2}$  of the glasses studied here increases with their total surface Na, K, Mg, and Ca content (Figure 2c). The  $\gamma_{\text{SO}_2}$  broadly exhibits a similar tendency (Figure 2d). This likely reflects a role of basic surface sites associated with these

elements in  $\text{SO}_2$  adsorption (e.g.,  $\text{SO}_{2(g)} + \text{Mg-OH}_{(s)} \rightarrow \text{Mg-OS-O}_2\text{-H}_{(s)}$ ) (Zhang et al., 2006). Accordingly,  $N_i^{\text{SO}_2}$  increases with the total basic site abundance on the glass samples as independently revealed by the strongly acidic probe gas trifluoroacetic acid (i.e.,  $N_i^{\text{TFA}}$ ) (Maters et al., 2016) (Figure S1). Since  $\text{SO}_2$  is a weakly acidic gas, its uptake is thought to occur on strongly basic sites representing a subset of all basic sites interacting with TFA and affiliated with alkali and alkaline earth metals at the surface. Semiquantitative comparison of these data suggests that strongly basic sites ( $N_i^{\text{SO}_2}$ ) make up ~20% of total basic sites ( $N_i^{\text{TFA}}$ ) on the glass samples (Figure S1).

Sulfur dioxide chemisorption at basic sites may involve reaction with oxide anions ( $\text{O}^{2-}$ ) or hydroxyl groups ( $\text{OH}^-$ ), leading to formation of surface S(IV) species (Goodman et al., 2001; Karge & Dalla Lana, 1984; Pacchioni et al., 1994; Waqif et al., 1992). Sulfite ( $\text{SO}_3^{2-}$ ) and bisulfite ( $\text{HSO}_3^-$ ) have been detected by various spectroscopic techniques on natural dust, mineral oxide, and aluminosilicate glass powders exposed to  $\text{SO}_2$  gas (e.g., Farges et al., 2009; Goodman et al., 2001; Ullerstam et al., 2002; Usher et al., 2002; Zhang et al., 2006). As volcanic glass and ash have been shown to contain basic surface sites (Maters et al., 2016),  $\text{SO}_2$  chemisorption forming  $\text{SO}_3^{2-}/\text{HSO}_3^-$  likely occurred on these materials in the Knudsen flow reactor. Importantly, no  $\text{SO}_2$  desorption was measured after stopping the gas flow and no secondary  $\text{SO}_2$  uptake was observed upon sample reexposure to the gas flow, indicating that  $\text{SO}_2$  uptake was irreversible on the glass and ash on the time-scale of our measurements. Aqueous leachates of the original glass samples and a subset of those exposed to  $\text{SO}_2$  support the formation of  $\text{SO}_3^{2-}$  on the latter, as dissolved  $\text{SO}_3^{2-}$  was not detected in leachates of the original glasses but was present in those of the exposed glasses (Text S3 and Table S6). Additionally, the rank of  $\text{SO}_3^{2-}$  concentrations measured in the exposed glass leachates follows the rank of  $N_i^{\text{SO}_2}$  values determined for the glass samples in the Knudsen flow reactor, i.e., trachybasalt > andesite > dacite > rhyolite (Figure 2a and Table S3).

Similar to the glass materials, the  $N_i^{\text{SO}_2}$  and  $\gamma_{\text{SO}_2}$  of the ash samples may show a dependence on total surface Na, K, Mg, and Ca content, although the relationship appears to be less clear (Figures 2c and 2d). A *t* test performed on the glass and ash  $N_i^{\text{SO}_2}$  data sets also confirms that the mean normalized  $\text{SO}_2$  uptake (i.e.,  $N_i^{\text{SO}_2}/\text{Na} + \text{K} + \text{Mg} + \text{Ca}$  content) for the glass samples exceeds that for the ash samples ( $P < 0.001$ ). Moreover, on the ash materials  $N_i^{\text{SO}_2}$  does not increase with the total basic site abundance as revealed by uptake of the probe gas TFA (i.e.,  $N_i^{\text{TFA}}$ ) (Maters et al., 2016) (Figure S1). Since  $\text{SO}_2$  and TFA react with basic sites of different strengths, this suggests that in contrast to the glasses, the relative abundance of strongly versus weakly basic sites varies widely for the ash specimens. This is exemplified by the dominance of weakly basic sites on Chaitén ash and strongly basic sites on Eyjafjallajökull ash (Figure S1). Altogether, these disparate trends in  $\text{SO}_2$  uptake by the glass and ash samples, including the overall lower  $N_i^{\text{SO}_2}$  of the latter (Table S3), may relate to the presence of crystalline mineral phases in ash and/or to the distinct surface generation and alteration histories of the glass and ash materials (Maters et al., 2016).

Farges et al. (2009) argue that  $\text{SO}_2$  adsorption on volcanic ash is most likely to occur on glassy regions of its surface, based on observations of higher  $\text{SO}_2$  uptake on  $\text{SiO}_2$  glass than on quartz. However, this conclusion neglects the importance of alkali and alkaline earth atoms in generating basic surface sites, and presently, we have no basis to infer that the abundances of strongly basic sites for  $\text{SO}_2$  uptake differ on amorphous versus crystalline aluminosilicates. While the  $\text{SO}_2$  uptake on the four ash samples studied here shows no trend according to bulk glass content (Figure S2), without knowledge of how amorphous and crystalline phases within ash are actually distributed at the solid surface, we can neither confirm nor refute an influence of crystallinity on  $\text{SO}_2$  uptake by ash.

The glass and ash also differ fundamentally in terms of prior ash interaction with acidic gases and condensate during transit through the volcanic plume/cloud. Partial removal/neutralization of basic surface sites (e.g., Digne et al., 2008; Zhang et al., 2002) and, relatedly, exposure to gaseous  $\text{SO}_2$  during the eruption probably explain the lower and more variable  $\text{SO}_2$  uptake on the natural ash compared to the synthetic glass in this study. Reaction with  $\text{SO}_2$  at high temperature in the plume produces ash surfaces bearing  $\text{SO}_4^{2-}$  salts (e.g.,  $\text{CaSO}_4$ ,  $\text{Na}_2\text{SO}_4$ ) (Ayris et al., 2013) and therefore likely containing fewer sites for additional  $\text{SO}_2$  uptake in the Knudsen flow reactor. Convincingly, aqueous leachates of the original ash samples indicate the presence of S species (e.g.,  $\text{SO}_4^{2-}$ ) already on the erupted material (Text S4 and Table S7). The remarkably high dissolved  $\text{SO}_4^{2-}$  content of the Chaitén ash leachate may point to extensive prior

ash-SO<sub>2</sub> interaction in the Chaitén plume. This could partly explain the particularly low relative abundance of strongly basic sites on Chaitén ash (Figure S1) and conforms with its low SO<sub>2</sub> uptake measured here (Table S3). Judeikis et al. (1978) similarly hypothesized that reaction of fly ash with SO<sub>2</sub> at high temperature within the coal-fired emission source lowers its capacity for subsequent experimental SO<sub>2</sub> uptake, i.e., compared to the same ash pre-rinsed to remove soluble S species. Thus, partial consumption of reactive sites on ash surfaces already near the point of emission may diminish heterogeneous SO<sub>2</sub> removal in the atmosphere.

#### 4.2. Ozone Uptake

As for SO<sub>2</sub> gas, all volcanic glass and ash samples were reactive toward O<sub>3</sub> gas (Table S4).

Neither the glass nor the ash show a relationship between  $N_i^{O_3}$  or  $\gamma_{O_3}$  and surface chemical composition (e.g., Figures 3a and 3b). Others have suggested a compositional influence on O<sub>3</sub> uptake by mineral oxides and natural dust, decreasing in the order Fe<sub>2</sub>O<sub>3</sub> > Al<sub>2</sub>O<sub>3</sub> > SiO<sub>2</sub> > kaolinite, with Saharan sand and Chinese loess near the lower end of this rank, although this trend is not well understood (Hanisch & Crowley, 2003; Michel et al., 2003; Suzuki et al., 1979). Reactive O<sub>3</sub> uptake on such substrates may consist of dissociative adsorption, possibly involving Lewis acid sites, resulting overall in catalytic O<sub>3</sub> decomposition and O<sub>2</sub> production (Bulanin et al., 1995; Golodets, 1983; Thomas et al., 1997). This reportedly proceeds by (i) relatively fast O<sub>3</sub> adsorption leading to surface bound O and gaseous O<sub>2</sub>, (ii) secondary O<sub>3</sub> adsorption forming surface bound peroxide (O<sub>2</sub><sup>2-</sup>) and gaseous O<sub>2</sub>, and finally, (iii) slow decomposition of surface bound O<sub>2</sub><sup>2-</sup> and/or recombination of two surface bound Os, resulting in O<sub>2</sub> desorption and hence, regeneration of reactive surface sites (Li et al., 1998; Li & Oyama, 1998).

There is no evidence of catalytic O<sub>3</sub> decomposition on the glass or ash here as all samples show finite reactivity toward O<sub>3</sub>, with surfaces saturating over the course of the experiments (e.g., Figure 1b). As observed for SO<sub>2</sub>, reaction of the glass and ash with O<sub>3</sub> was irreversible on the timescale of our measurements, with neither desorption nor secondary uptake of O<sub>3</sub> measured upon stopping and restarting the gas flow. Determination of O<sub>3</sub>/O<sub>2</sub> ratios by monitoring O<sub>3</sub> loss and O<sub>2</sub> evolution, i.e., to assess consistency with the expected overall stoichiometry of catalytic O<sub>3</sub> decomposition (2O<sub>3(g)</sub> → 3O<sub>2(g)</sub>), was unfortunately hindered by the high O<sub>2</sub> background in the Knudsen reactor (see Text S5). It is possible that regeneration of reactive surface sites for O<sub>3</sub> uptake on the glass and ash was not observed within the measurement timescale due to slow formation of the O<sub>2</sub><sup>2-</sup> intermediate and desorption of O<sub>2</sub> from these sites (Hanisch & Crowley, 2003; Li & Oyama, 1998). Alternatively, Karagulian and Rossi (2006) suggest that non-catalytic O<sub>3</sub> interaction with various mineral and dust substrates may proceed with irreversible O<sub>3</sub> adsorption forming a surface adduct without subsequently releasing O<sub>2</sub>.

Ozone is a strong oxidizing agent which has been applied as a probe gas for reducing functional groups on various solid substrates (e.g., Setyan et al., 2010a, 2010b; Tapia et al., 2015, 2016), and we similarly attribute its uptake on the glass and ash material to adsorption on reducing surface sites (Maters et al., 2016). These sites may include oxygen deficiencies in the anionic oxide (O<sup>2-</sup>) network at the solid-gas interface (Diebold, 2003) and transition metal atoms (e.g., Fe) in their lower valence state (e.g., Fe<sup>2+</sup>) present in varying abundance on the aluminosilicate samples (Maters et al., 2016). Irreversible O<sub>3</sub> adsorption on such sites may involve insertion of an O or O<sub>2</sub> into an oxygen vacancy and/or interfacial Fenton-like chemistry, leading to formation of peroxide, superoxide, hydroxyl radical, and/or ferryl species at the surface (Enami et al., 2014; He et al., 2016; Li et al., 1998). Further research is necessary to elucidate the precise O<sub>3</sub> uptake mechanism on the glass and ash material studied here.

As shown by Maters et al. (2016), the typically lower  $N_i^{O_3}$  values of the ash compared to the glass (Figure 3a and Table S4) conform with ash surfaces being relatively less reducing, likely due to exposure to an oxidizing mixture of hot gases and atmospheric air >600°C in the volcanic plume. The exceptional  $N_i^{O_3}$  value displayed by Pinatubo ash, an order of magnitude higher than those of the other ash samples, may reflect a greater abundance of reducing surface sites provided by micrometric pyrite (FeS<sub>2</sub>) in this ash (Maters et al. 2016). Notably, the  $\gamma_{O_3}$  values of Pinatubo and Eyjafjallajökull ash were up to 6 times higher than those of the glass and other ash samples (Figure 3b and Table S4). This observation could also relate to the presence of FeS<sub>2</sub> in Pinatubo ash and Fe(II)-bearing saponite (general formula Ca<sub>0.25</sub>(Mg,Fe)<sub>3</sub>(Si,Al)<sub>4</sub>O<sub>10</sub>(OH)<sub>2</sub>·nH<sub>2</sub>O) in

Eyjafjallajökull ash (Paque et al., 2016), providing reducing surface sites for rapid uptake of  $O_3$ , although variation in  $\gamma$  values must be interpreted with caution and additional surface molecular/structural analyses would be needed to confirm this hypothesis.

### 4.3. Interaction Between Sulfur Dioxide and Ozone Uptake

For our glass samples,  $N_i^{O_3}$  was consistently slightly higher after exposure to  $SO_2$  (Figure 4a and Table S5), suggesting interaction of  $O_3$  with adsorbed S species on glass surfaces. Previous studies of  $SO_2$  uptake on mineral dust (e.g., Chinese loess and Saharan sand) and its component oxides (e.g., MgO,  $CaCO_3$ ,  $Al_2O_3$ ,  $Fe_2O_3$ , and  $SiO_2$ ) have reported oxidation of chemisorbed  $SO_3^{2-}/HSO_3^-$  to  $SO_4^{2-}/HSO_4^-$  in the presence of an oxidizing agent (e.g.,  $O_3$ ,  $NO_2$ , and  $O_2$  in air albeit more slowly) (Fu et al., 2007; Li et al., 2006; Ullerstam et al., 2002, 2003; Usher et al., 2002). Accordingly, basic sites reacting with  $SO_2$  (forming adsorbed S(IV) species) on our glasses may be converted into reducing (oxidizable) sites (Ziolek et al., 1996), in addition to those already present, hence leading to detection of an increased abundance of reducing sites upon interaction with  $O_3$ . For the ash samples in contrast, there was no consistent difference in  $N_i^{O_3}$  between the original versus the  $SO_2$ -exposed materials (Figure 4a and Table S5). This observation may be attributable to prior ash interaction with  $SO_2$  in the volcanic plume/cloud; the presence of adsorbed S species already on “fresh” ash likely minimized an influence of additional  $SO_2$  exposure (i.e., in the Knudsen flow reactor) on subsequent  $O_3$  uptake by the ash. However, Pinatubo ash showed an exceptional fourfold decrease in  $N_i^{O_3}$  following  $SO_2$  exposure (Figure 4a), which may point to the existence of a poisoning effect of  $SO_2$  on surface sites for  $O_3$  adsorption on pyrite. Similarly, we note a sixfold decrease in  $\gamma_{O_3}$  for the dacite glass after  $SO_2$  exposure (Figure 4b), while no significant effect of  $SO_2$  exposure on  $\gamma_{O_3}$  for any of the other glass or ash samples is apparent. Further investigation is necessary to shed light on the factors underlying this observed heterogeneity in ash and glass surface reactivity.

Overall, we infer that  $SO_4^{2-}/HSO_4^-$  may be emplaced on sample surfaces at ambient temperature by adsorption of  $SO_2$  gas (forming  $SO_3^{2-}/HSO_3^-$ ) followed by interaction with  $O_3$  gas (Li et al., 2006). This would be expected to occur on airborne ash since particles exposed to  $SO_2$ , coemitted during the eruption and present in the background atmosphere, are in contact with oxidizing agents from the moment of air entrainment in the volcanic plume/cloud. Sulfate is nearly ubiquitous on fresh ash surfaces (Witham et al., 2005) and has similarly been measured in aqueous leachates of the original ash samples studied here (Table S7). It is possible that this surface  $SO_4^{2-}$  derives in part from ash-gas interactions in the atmosphere in addition to ash-gas/condensate interactions during transit through distinct temperature-dependent reaction zones in the eruption plume/cloud (e.g., Ayris et al., 2013; Delmelle et al., 2007; Óskarsson, 1980; Rose, 1977; Taylor & Stoiber, 1973).

## 5. Implications and Conclusions

The reactive uptake of gaseous  $SO_2$  and  $O_3$  on ash and glass at ambient temperature, quantified here for the first time using a Knudsen flow reactor, likely involves  $SO_2$  adsorption at basic sites and  $O_3$  adsorption at reducing sites on the aluminosilicate surfaces. A lower  $SO_2$  uptake on ash relative to glass is attributable to prior exposure of ash to acidic gases/condensates (including  $SO_2$ ) within the eruption plume/cloud. Similarly, a generally lower  $O_3$  uptake on ash compared to glass may relate to oxidation of ash surfaces in the high-temperature water-rich volcanic plume.

Irreversible uptake of  $SO_2$  in the amount of 0.8 to 1  $mg\ m^{-2}$  on glass powders has been reported by Schmauss and Keppler (2014), corresponding to 10 to 120 and 40 to 1600 times the  $N_i^{SO_2}$  values obtained here for the glass and ash samples, respectively. However, those authors' measurements were acquired over hours at  $SO_2$  partial pressures ( $>10$  Pa) that would not be sustained for longer than minutes due to turbulent mixing of the volcanic plume/cloud with air (Sparks et al., 1997), and that greatly exceed the atmospherically representative  $SO_2$  partial pressures used in the present study ( $<0.01$  Pa). While our measurements suggest that partial saturation of ash surfaces in the volcanic plume/cloud may diminish ash reactivity toward  $SO_2$  in the ambient atmosphere, the ranges of  $N_i^{SO_2}$  and  $\gamma_{SO_2}$  values exhibited by the glass and ash are comparable to those reported for oxide powders, mineral dust, and even liquid aerosols (Table S8).

Background O<sub>3</sub> depletion observed in some volcanic plumes/clouds is generally regarded as resulting from catalytic reaction with halogen radicals (Roberts et al., 2009; von Glasow, 2010). Using a  $\gamma_{\text{O}_3}$  of  $10^{-5}$  (taken as a value for mineral dust over its BET surface area), Vance et al. (2010) discounted heterogeneous reaction with ash as a viable O<sub>3</sub> loss mechanism. However, we measured a  $\gamma_{\text{O}_3}$  range of  $10^{-3}$  to  $10^{-2}$  for volcanic ash over the geometric surface area initially probed by the gas, meaning that significantly less erupted ash than estimated by Vance et al. (2010) would be required to sustain heterogeneous O<sub>3</sub> removal consistent with the reductions observed in the field (see Text S6).

Based on our N<sub>i</sub><sup>O<sub>3</sub></sup> values, and assuming “light” or “intense” ash concentrations of 0.1 or 5 g m<sup>-3</sup> in an ash plume/cloud (Marzano et al., 2010), we estimate that O<sub>3</sub> uptake on ash surfaces could deplete 0.1 to 4.6% or 4.6 to 230% of the background tropospheric O<sub>3</sub> concentration, respectively (see Text S7). These ranges are comparable to O<sub>3</sub> depletions attributed to destruction by volcanic halogen-derived reactive species (Surl et al., 2015; Vance et al., 2010). Interestingly, de Reus et al. (2000) measured a distinct anticorrelation between particle and O<sub>3</sub> concentrations in air parcels of a mineral dust plume. A similar effect may occur in the case of an ash plume/cloud since the ranges of N<sub>i</sub><sup>O<sub>3</sub></sup> and  $\gamma_{\text{O}_3}$  values displayed by the glass and ash are comparable to those reported for oxide powders, mineral dust, and liquid aerosols (Table S9).

It remains to be verified whether ash surfaces can take part in catalytic decomposition of O<sub>3</sub> on timescales longer than those of our experiments, thereby increasing its removal from the atmosphere (Pitcock, 1965). Remarkably, the ash samples show highly variable reactivities toward O<sub>3</sub>, with uptake values of Pinatubo (N<sub>i</sub><sup>O<sub>3</sub></sup> and  $\gamma_{\text{O}_3}$ ) and Eyjafjallajökull ( $\gamma_{\text{O}_3}$ ) ash exceeding those of Tungurahua and Chaitén ash. These observations highlight a great heterogeneity in ash surface reactivity, implying that some eruptions may release ash particles with a strong potential for heterogeneous reaction with atmospheric O<sub>3</sub>. Additional studies are needed to unravel what may control the variability and disparity in N<sub>i</sub><sup>O<sub>3</sub></sup> and  $\gamma_{\text{O}_3}$  values of ash from different eruptions.

Our results also suggest that O<sub>3</sub> may facilitate oxidation of surface adsorbed S(IV) species, although more experiments are necessary to confirm this reaction. If so, SO<sub>2</sub> adsorption on ash surfaces in the cool volcanic cloud or atmosphere could generate additional reducing sites on the ash and thereby enhance its capacity to react with O<sub>3</sub>. Moreover, this oxidation pathway (i.e., SO<sub>3</sub><sup>2-</sup>/HSO<sub>3</sub><sup>-</sup> to SO<sub>4</sub><sup>2-</sup>/HSO<sub>4</sub><sup>-</sup>) on ash surfaces would effectively minimize SO<sub>2</sub> desorption back into the gas phase (Adams et al., 2005), accordingly facilitating the role of ash as a sink for SO<sub>2</sub>. In the atmosphere, adsorbed S(IV) species may be oxidized by O<sub>2</sub> as well via coupling with Fe<sup>3+</sup> reduction to Fe<sup>2+</sup> (Fu et al., 2007) in the aluminosilicate surfaces. While this mechanism likely prevails in the aqueous phase (Brandt & van Eldik, 1995), Fenton-like chemistry involving Fe<sup>3+</sup>/Fe<sup>2+</sup>-catalyzed redox chain reactions may take place at the solid-gas interface using strongly bound H<sub>2</sub>O (He et al., 2016) and importantly could lead to regeneration of surface sites for atmospheric SO<sub>2</sub> withdrawal.

Overall, our study demonstrates that volcanic ash is reactive toward gaseous SO<sub>2</sub> and O<sub>3</sub> at ambient temperature and hence merits recognition as an atmospheric chemical agent alongside of volcanogenic gases/aerosols as well as mineral dust. We present benchmark experimental data on ash-gas reactivity which can also aid in improving quantification of heterogeneous reactions in atmospheric and climate models.

#### Acknowledgments

P.D. gratefully acknowledges support from the FNRS (MIS-Ulysse grant F.6001.11). E.C.M. benefitted from a FNRS studentship (MIS-Ulysse grant F.6001.11, 2012–2014 and Mandat d'Aspirante grant FC.88010, 2015). M.J.R. thanks the Paul Scherrer Institute, namely, Urs Baltensperger and Alexander Wokaun, for providing the laboratory infrastructure enabling the uptake measurements. We are grateful for the assistance of C. Givron with leachate analysis, P. Eloy with XPS analysis, and A. Vandeuken with statistical analysis. We thank E. Gaigneaux and J. Schnee for access to and aid with the specific surface area analyzer. The data used in this study are listed in the references, Figures 1–4, S1 and S2, and Tables 1 and S1–S9 in the manuscript and the supporting information.

#### References

- Adams, J. W., Rodriguez, D., & Cox, R. A. (2005). The uptake of SO<sub>2</sub> on Saharan dust: A flow tube study. *Atmospheric Chemistry and Physics*, 5(10), 2679–2689. <https://doi.org/10.5194/acp-5-2679-2005>
- Ammann, M., Cox, R. A., Crowley, J. N., Jenkin, M. E., Mellouki, A., Rossi, M. J., ... Wallington, T. J. (2013). Evaluated kinetic and photochemical data for atmospheric chemistry: Volume VI—Heterogeneous reactions with liquid substrates. *Atmospheric Chemistry and Physics*, 13(16), 8045–8228. <https://doi.org/10.5194/acp-13-8045-2013>
- Ayris, P. M., Lee, A. F., Wilson, K., Kueppers, U., Dingwell, D. B., & Delmelle, P. (2013). SO<sub>2</sub> sequestration in large volcanic eruptions: High-temperature scavenging by tephra. *Geochimica et Cosmochimica Acta*, 110(1), 58–69. <https://doi.org/10.1016/j.gca.2013.02.018>
- Brandt, C., & van Eldik, R. (1995). Transition metal-catalyzed oxidation of sulfur(IV) oxides. Atmospheric-relevant processes and mechanisms. *Chemical Reviews*, 95(1), 119–190. <https://doi.org/10.1021/cr00033a006>
- Brasseur, G. P., Granier, C., & Walters, S. (1990). Future changes in stratospheric ozone and the role of heterogeneous chemistry. *Nature*, 348(6285), 626–628. <https://doi.org/10.1038/348626a0>
- Bulanin, K. M., Lavalley, J. C., & Tsyganenko, A. A. (1995). IR spectra of adsorbed ozone. *Colloids and Surfaces A: Physicochemical and Engineering Aspects*, 101(2–3), 153–158. [https://doi.org/10.1016/0927-7757\(95\)03130-6](https://doi.org/10.1016/0927-7757(95)03130-6)
- Caloz, F., Fenter, F. F., Tabor, K. D., & Rossi, M. J. (1997). Paper I: Design and construction of a Knudsen-cell reactor for the study of heterogeneous reactions over the temperature range 130–750 K: Performance and limitations. *The Review of Scientific Instruments*, 68(8), 3172–3179. <https://doi.org/10.1063/1.114826>

- Chao, T. T., & Sanzalone, R. F. (1992). Decomposition techniques. *Journal of Geochemical Exploration*, 44(1), 65–106. [https://doi.org/10.1016/0375-6742\(92\)90048-D](https://doi.org/10.1016/0375-6742(92)90048-D)
- Delmelle, P., Lambert, M., Dufrière, Y., Gerin, P., & Óskarsson, N. (2007). Gas/aerosol-ash interaction in volcanic plumes: New insights from surface analysis of fine ash particles. *Earth and Planetary Science Letters*, 259(1–2), 159–170. <https://doi.org/10.1016/j.epsl.2007.04.052>
- Delmelle, P., Villieras, F., & Pelletier, M. (2005). Surface area, porosity and water adsorption properties of fine volcanic ash particles. *Bulletin of Volcanology*, 67(2), 160–169. <https://doi.org/10.1007/s00445-004-0370-x>
- de Reus, M., Dentener, F., Thomas, A., Borrmann, S., Ström, J., & Lelieveld, J. (2000). Airborne observations of dust aerosol over the North Atlantic Ocean during ACE 2: Indications for heterogeneous ozone destruction. *Journal of Geophysical Research*, 105(D12), 15,263–15,275. <https://doi.org/10.1029/2000JD900164>
- Diebold, U. (2003). The surface science of titanium dioxide. *Surface Science Reports*, 48(5), 53–229. [https://doi.org/10.1016/S0167-5729\(02\)00100-0](https://doi.org/10.1016/S0167-5729(02)00100-0)
- Digne, M., Raybaud, P., Sautet, P., Guillaume, D., & Toulhoat, H. (2008). Atomic scale insights on chlorinated  $\gamma$ -alumina surfaces. *Journal of the American Chemical Society*, 130(33), 11,030–11,039. <https://doi.org/10.1021/ja8019593>
- Durant, A. J., Bonadonna, C., & Horwell, C. J. (2010). Atmospheric and environmental impact of volcanic particulates. *Elements*, 6(4), 235–240. <https://doi.org/10.2113/gselements.6.4.235>
- Enami, S., Sakamoto, Y., & Colussi, A. J. (2014). Fenton chemistry at aqueous interfaces. *Proceedings of the National Academy of Sciences of the United States of America*, 111(2), 623–628. <https://doi.org/10.1073/pnas.1314885111>
- Farges, F., Keppler, H., Flank, A. -M., & Lagarde, P. (2009). Sulfur K-edge XANES study of S sorbed onto volcanic ashes. *Journal of Physics Conference Series*, 190(1), 012177. <https://doi.org/10.1088/1742-6596/190/1/012177>
- Fu, H., Wang, X., Wu, H., Yin, Y., & Chen, J. (2007). Heterogeneous uptake and oxidation of SO<sub>2</sub> on iron oxides. *Journal of Physical Chemistry C*, 111(16), 6077–6085. <https://doi.org/10.1021/jp070087b>
- Golden, D. M., Spokes, G. N., & Benson, S. W. (1973). Very low-pressure pyrolysis (VLPP): A versatile kinetic tool. *Angewandte Chemie, International Edition*, 12(7), 534–546. <https://doi.org/10.1002/anie.197305341>
- Golodets, G. I. (1983). *Heterogeneous catalytic reactions involving molecular oxygen*. Oxford: Butterworth-Heinemann Limited.
- Goodman, A. L., Li, P., Usher, C. R., & Grassian, V. H. (2001). Heterogeneous uptake of sulfur dioxide on aluminum and magnesium oxide particles. *The Journal of Physical Chemistry, A*, 105(25), 6109–6120. <https://doi.org/10.1021/jp004423z>
- Hanisch, F., & Crowley, J. N. (2003). Ozone decomposition on Saharan dust: An experimental investigation. *Atmospheric Chemistry and Physics*, 3(1), 119–130. <https://doi.org/10.5194/acp-3-119-2003>
- Harris, D. M., Rose, W. I., Jr., Roe, R., Thompson, M. R., Lipman, P. W., & Mullineaux, D. R. (1981). *Radar Observations of Ash Eruptions, the 1980 Eruptions of Mount St. Helens, Washington U.S. Geological Survey Professional Paper 1250* (Vol. 1250, pp. 323–333). Reston, VA: U. S. Geological Survey.
- He, J., Yang, X., Men, B., & Wang, D. (2016). Interfacial mechanisms of heterogeneous Fenton reactions catalyzed by iron-based materials: A review. *Journal of Environmental Sciences*, 39, 97–109. <https://doi.org/10.1016/j.jes.2015.12.003>
- Judeikis, H. S., Stewart, T. B., & Wren, A. G. (1978). Laboratory studies of heterogeneous reactions of SO<sub>2</sub>. *Atmospheric Environment*, 12(8), 1633–1641. [https://doi.org/10.1016/0004-6981\(78\)90312-8](https://doi.org/10.1016/0004-6981(78)90312-8)
- Karagulian, F., & Rossi, M. J. (2006). The heterogeneous decomposition of ozone on atmospheric mineral dust surrogates at ambient temperature. *International Journal of Chemical Kinetics*, 38(6), 407–419. <https://doi.org/10.1002/kin.20175>
- Karge, H. G., & Dalla Lana, I. G. (1984). Infrared studies of SO<sub>2</sub> adsorption on a Claus catalyst by selective poisoning of sites. *The Journal of Physical Chemistry*, 88(8), 1538–1543. <https://doi.org/10.1021/j150652a019>
- Koyaguchi, T. (1996). Volume estimation of tephra fall-deposits from the June 15, 1991, eruption of Mount Pinatubo by theoretical and geological methods. In C. G. Newhall, & R. S. Punongbayan (Eds.), *Fire and Mud: Eruptions and lahars of Mount Pinatubo, Philippines* (pp. 583–600). Washington: Phivolcs and United States Geological Survey.
- Le Maitre, R. W., Streckeisen, A., Zanettin, B., Le Bas, M. J., Bonin, B., & Bateman, P. (2002). *Igneous rocks: A classification and glossary of terms, recommendations of the international union of geological sciences subcommission on the systematics of igneous rocks*. Cambridge: Cambridge Univ. Press.
- Li, L., Chen, Z. M., Zhang, Y. H., Zhu, T., Li, J. L., & Ding, J. (2006). Kinetics and mechanism of heterogeneous oxidation of sulfur dioxide by ozone on surface of calcium carbonate. *Atmospheric Chemistry and Physics*, 6(9), 2453–2464. <https://doi.org/10.5194/acp-6-2453-2006>
- Li, W., & Oyama, S. T. (1998). Mechanism of ozone decomposition on a manganese oxide catalyst. 2. Steady-state and transient kinetic studies. *Journal of the American Chemical Society*, 120(35), 9047–9052. <https://doi.org/10.1021/ja9814422>
- Li, W., Gibbs, G. V., & Oyama, S. T. (1998). Mechanism of ozone decomposition on a manganese oxide catalyst. 1. In situ Raman spectroscopy and ab initio molecular orbital calculations. *Journal of the American Chemical Society*, 120(35), 9041–9046. <https://doi.org/10.1021/ja981441+>
- Magi, L., Schweitzer, F., Pallares, C., Cherif, S., Mirabel, P., & George, C. (1997). Investigation of the uptake rate of ozone and methyl hydroperoxide by water surfaces. *The Journal of Physical Chemistry*, 101(27), 4943–4949. <https://doi.org/10.1021/jp970646m>
- Marzano, F. S., Barbieri, S., Picciotti, E., & Karlsdóttir, S. (2010). Monitoring subglacial volcanic eruption using ground-based C-band radar imagery. *IEEE Transactions on Geoscience and Remote Sensing*, 48(1), 403–414. <https://doi.org/10.1109/TGRS.2009.2024933>
- Maters, E. C., Delmelle, P., Rossi, M. J., Ayris, P. M., & Bernard, A. (2016). Controls on volcanic ash surface reactivity investigated with probe gases. *Earth and Planetary Science Letters*, 450, 254–262. <https://doi.org/10.1016/j.epsl.2016.06.044>
- Matsuki, A., Iwasaka, Y., Shi, G., Zhang, D., Trochkin, D., Yamada, M., ... Nakata, H. (2005). Morphological and chemical modification of mineral dust: Observational insight into the heterogeneous uptake of acidic gases. *Geophysical Research Letters*, 32, L22806. <https://doi.org/10.1029/2005GL024176>
- Michel, A. E., Usher, C. R., & Grassian, V. H. (2002). Heterogeneous and catalytic uptake of ozone on mineral oxides and dusts: A Knudsen cell investigation. *Geophysical Research Letters*, 29(14), 1665. <https://doi.org/10.1029/2002GL014896>
- Michel, A. E., Usher, C. R., & Grassian, V. H. (2003). Reactive uptake of ozone on mineral oxides and mineral dusts. *Atmospheric Environment*, 37(23), 3201–3211. [https://doi.org/10.1016/S1352-2310\(03\)00319-4](https://doi.org/10.1016/S1352-2310(03)00319-4)
- Niemeier, U., Timmreck, C., Graf, H.-F., Kinne, S., Rast, S., & Self, S. (2009). Initial fate of fine ash and sulfur from large volcanic eruptions. *Atmospheric Chemistry and Physics*, 9(22), 9043–9057. <https://doi.org/10.5194/acp-9-9043-2009>
- Óskarsson, N. (1980). The interaction between volcanic gases and tephra: Fluorine adhering to tephra of the 1970 Hekla eruption. *Journal of Volcanology and Geothermal Research*, 8(2–4), 251–266. [https://doi.org/10.1016/0377-0273\(80\)90107-9](https://doi.org/10.1016/0377-0273(80)90107-9)

- Pacchioni, G., Clotet, A., & Ricart, J. M. (1994). A theoretical study of the adsorption and reaction of SO<sub>2</sub> at surface and step sites of the MgO(100) surface. *Surface Science*, 315(3), 337–350. [https://doi.org/10.1016/0039-6028\(94\)90137-6](https://doi.org/10.1016/0039-6028(94)90137-6)
- Paque, M., Detienne, M., Maters, E. C., & Delmelle, P. (2016). Smectites and zeolites in ash from the 2010 summit eruption of Eyjafjallajökull volcano, Iceland. *Bulletin of Volcanology*, 78(61), 1–10. <https://doi.org/10.1007/s00445-016-1056-x>
- Penner, J. E., Andreae, M., Annegarn, H., Barrie, L., Feichter, J., Hegg, D., ... Pitari, G. (2001). Aerosols, their direct and indirect effects. In J. T. Houghton et al. (Eds.), *Climate Change 2001: The Scientific Basis*, Contribution of Working Group I to the Third Assessment Report of the Intergovernmental Panel on Climate Change (pp. 290–347). New York, NY: Cambridge Univ. Press.
- Pittock, A. B. (1965). Possible destruction of ozone by volcanic material at 50 mbar. *Nature*, 207, 1.
- Roberts, T. J., Braban, C. F., Martin, R. S., Oppenheimer, C., Adams, J. W., Cox, R. A., ... Griffiths, P. T. (2009). Modelling reactive halogen formation and ozone depletion in volcanic plumes. *Chemical Geology*, 263(1–4), 151–163. <https://doi.org/10.1016/j.chemgeo.2008.11.012>
- Robock, A. (2000). Volcanic eruptions and climate. *Reviews of Geophysics*, 38(2), 191–219. <https://doi.org/10.1029/1998RG000054>
- Rose, W. I. (1977). Scavenging of volcanic aerosol by ash: Atmospheric and volcanologic implications. *Geology*, 5(10), 621–624. [https://doi.org/10.1130/0091-7613\(1977\)5<621:SOVABA>2.0.CO;2](https://doi.org/10.1130/0091-7613(1977)5<621:SOVABA>2.0.CO;2)
- Schmauss, D., & Keppler, H. (2014). Adsorption of sulfur dioxide on volcanic ashes. *American Mineralogist*, 99(5–6), 1085–1094. <https://doi.org/10.2138/am.2014.4656>
- Seinfeld, J. H., & Pandis, S. N. (2016). *Atmospheric chemistry and physics: From air pollution to climate change* (3rd ed., pp. 1152). New Jersey: John Wiley.
- Seisel, S., Keil, T., Lian, Y., & Zellner, R. (2006). Kinetics of the uptake of SO<sub>2</sub> on mineral oxides: Improved initial uptake coefficient at 298 K from pulsed Knudsen cell experiments. *International Journal of Chemical Kinetics*, 38(4), 242–249. <https://doi.org/10.1002/kin.20148>
- Seisel, S., Keil, T., & Zellner, R. (2009). The uptake of SO<sub>2</sub> on α-Fe<sub>2</sub>O<sub>3</sub> and mineral dust surfaces in the temperature range 250 K to 600 K. *Zeitschrift für Physikalische Chemie*, 223(12), 1477–1495. <https://doi.org/10.1524/zpch.2009.5499>
- Setyan, A., Sauvain, J.-J., Guillemin, M., Riediker, M., Demirdjian, B., & Rossi, M. J. (2010a). Probing functional groups at the gas-aerosol interface using heterogeneous titration reactions: A tool for predicting aerosol health effects?. *Physical Chemistry Chemical Physics*, 11(18), 3823–3835. <https://doi.org/10.1002/cphc.201000490>
- Setyan, A., Sauvain, J.-J., Guillemin, M., Riediker, M., & Rossi, M. J. (2010b). The surface chemical reactivity of combustion particles. In G. I. Stoev (Ed.), *Heterogeneous Combustion* (pp. 111–137). Hauppauge: Nova Science Publishers.
- Sparks, R. S. J., Bursik, M. I., Carey, S. N., Gilbert, J. S., Glaze, L. S., Sigurdsson, H., & Woods, A. W. (1997). *Volcanic plumes* (pp. 557). New York: John Wiley and Sons.
- Stewart, C., Horwell, C., Plumlee, G., Cronin, S., Delmelle, P., Baxter, P., ... Oppenheimer, C. (2013). *Protocol for analysis of volcanic ash samples for assessment of hazards from leachable elements* (pp. 21). International Volcanic Health Hazard Network (IVHHN).
- Surl, L., Donohoue, D., Aiuppa, A., Bobrowski, N., & von Glasow, R. (2015). Quantification of the depletion of ozone in the plume of Mount Etna. *Atmospheric Chemistry and Physics*, 15(5), 2613–2628. <https://doi.org/10.5194/acp-15-2613-2015>
- Suzuki, S., Hori, Y., & Koga, O. (1979). Decomposition of ozone on natural sand. *Bulletin of the Chemical Society of Japan*, 52(10), 3103–3104. <https://doi.org/10.1246/bcsj.52.3103>
- Tapia, A., Salgado, M. S., Martín, M. P., Sánchez-Valdepeñas, J., Rossi, M. J., & Cabañas, B. (2015). The use of heterogeneous chemistry for the characterization of functional groups at the gas/particle interface of soot from a diesel engine at a particular running condition. *Environmental Science and Pollution Research*, 22(7), 4863–4872. <https://doi.org/10.1007/s11356-014-2976-7>
- Tapia, A., Salgado, M. S., Martín, M. P., Lapuerta, M., Rodríguez-Fernández, J., Rossi, M. J., & Cabañas, B. (2016). Characterization of the gas-particle interface of soot sampled from a diesel engine using a titration method. *Environmental Science and Technology*, 50(6), 2946–2955. <https://doi.org/10.1021/acs.est.5b05531>
- Taylor, P. S., & Stoiber, R. E. (1973). Soluble material on ash from active Central American volcanoes. *Geological Society of America Bulletin*, 84(3), 1031–1042. [https://doi.org/10.1130/0016-7606\(1973\)84<1031:SMOFAA>2.0.CO;2](https://doi.org/10.1130/0016-7606(1973)84<1031:SMOFAA>2.0.CO;2)
- Thomas, K., Hoggan, P. E., Marley, L., Lamotte, J., & Lavalley, J. C. (1997). Experimental and theoretical study of ozone adsorption on alumina. *Catalysis Letters*, 46(1), 77–82. <https://doi.org/10.1023/A:1019017123596>
- Ullerstam, M., Johnson, M. S., Vogt, R., & Ljungström, E. L. (2003). DRIFTS and Knudsen cell study of the heterogeneous reactivity of SO<sub>2</sub> and NO<sub>2</sub> on mineral dust. *Atmospheric Chemistry and Physics*, 3(6), 2043–2051. <https://doi.org/10.5194/acp-3-2043-2003>
- Ullerstam, M., Vogt, R., Langer, S., & Ljungström, E. (2002). The kinetics and mechanism of SO<sub>2</sub> oxidation by O<sub>3</sub> on mineral dust. *Physical Chemistry Chemical Physics*, 4(19), 4694–4699. <https://doi.org/10.1039/b203529b>
- Usher, C. R., Al-Hosney, H., Carlos-Cuellar, S., and V. H. Grassian (2002). A laboratory study of the heterogeneous uptake and oxidation of sulfur dioxide on mineral dust particles. *Journal of Geophysical Research*, 107(D23), 4713. <https://doi.org/10.1029/2002JD002051>
- Usher, C. R., Michel, A. E., & Grassian, V. H. (2003). Reactions on mineral dust. *Chemical Reviews*, 103(12), 4883–4940. <https://doi.org/10.1021/cr020657y>
- Utter, R. G., Burkholder, J. B., Howard, C. J., & Ravishankara, A. R. (1992). Measurement of the mass accommodation coefficient of ozone on aqueous surfaces. *The Journal of Physical Chemistry*, 96(12), 4973–4979. <https://doi.org/10.1021/j100191a045>
- Vance, A., McGonigle, A. J. S., Aiuppa, A., Stith, J. L., Turnbull, K., & von Glasow, R. (2010). Ozone depletion in tropospheric volcanic plumes. *Geophysical Research Letters*, 37, L22802. <https://doi.org/10.1029/2010GL044997>
- Vernier, J.-P., Fairlie, T. D., Deshler, T., Natarajan, M., Knepp, T., Foster, K., ... Treppe, C. (2016). In situ and space-based observations of the Kelud volcanic plume: The persistence of ash in the lower stratosphere. *Journal of Geophysical Research: Atmospheres*, 121, 11,104–11,118. <https://doi.org/10.1002/2016JD025344>
- von Glasow, R. (2010). Atmospheric chemistry in volcanic plumes. *Proceedings of the National Academy of Sciences of the United States of America*, 107(15), 6594–6599. <https://doi.org/10.1073/pnas.0913164107>
- von Glasow, R., Bobrowski, N., & Kern, C. (2009). The effects of volcanic eruptions on atmospheric chemistry. *Chemical Geology*, 263(1–4), 131–142. <https://doi.org/10.1016/j.chemgeo.2008.08.020>
- Waqif, M., Saad, A. M., Bensitel, M., Bachelier, J., Saur, O., & Lavalley, J.-C. (1992). Comparative study of SO<sub>2</sub> adsorption on metal oxides. *Journal of the Chemical Society, Faraday Transactions*, 88(19), 2931–2936. <https://doi.org/10.1039/FT9928802931>
- Witham, C. S., Oppenheimer, C., & Horwell, C. J. (2005). Volcanic ash-leachates: A review and recommendations for sampling methods. *Journal of Volcanology and Geothermal Research*, 141(3–4), 299–326. <https://doi.org/10.1016/j.jvolgeores.2004.11.010>
- Wurzler, S., Reisin, T. G., & Levin, Z. (2000). Modification of mineral dust particles by cloud processing and subsequent effects on drop size distributions. *Journal of Geophysical Research*, 105(D4), 4501–4512. <https://doi.org/10.1029/1999JD900980>

- Zhang, W., Sun, M., & Prins, R. (2002). Multinuclear MAS NMR identification of fluorine species on the surface of fluorinated  $\gamma$ -alumina. *The Journal of Physical Chemistry B*, 106(45), 11,805–11,809. <https://doi.org/10.1021/jp0212489>
- Zhang, X., Guosghun, Z., Chen, J., Wang, Y., Wang, X., An, Z., & Zhang, P. (2006). Heterogeneous reactions of sulfur dioxide on typical mineral particles. *The Journal of Physical Chemistry B*, 110(25), 12,588–12,596. <https://doi.org/10.1021/jp0617773>
- Ziolek, M., Kujawa, J., Saur, O., Aboulayt, A., & Lavalley, J. C. (1996). Influence of sulfur dioxide adsorption on the surface properties of metal oxides. *Journal of Molecular Catalysis A: Chemical*, 112(1), 125–132.